http://dx.doi.org/10.5012/bkcs.2013.34.1.59

Effect of Calcination Temperature on the Structure and Electrochemical Performance of $LiMn_{1.5}Ni_{0.5}O_4$ Cathode Materials

Seo Hee Ju and Dong-Won Kim*

*Department of Chemical Engineering, Hanyang University, Seoul 133-791, Korea. *E-mail: dongwonkim@hanyang.ac.kr*
Received September 3, 2012, Accepted October 2, 2012

Spinel $LiMn_{1.5}Ni_{0.5}O_4$ cathode powders with different morphologies were synthesized by a co-precipitation method using oxalic acid. The calcination temperature affected the morphologies, crystalline structure and electrochemical properties of the $LiMn_{1.5}Ni_{0.5}O_4$ powders. The $LiMn_{1.5}Ni_{0.5}O_4$ powders obtained at a calcination temperature of 850 °C exhibited the highest initial discharge capacity with good capacity retention and high rate capability.

Key Words : Cathode, Lithium nickel manganese oxide, Lithium-ion battery, Calcination temperature, Electrochemical performance

Introduction

Lithium-ion batteries are attractive power sources for portable electronic devices, electric vehicles and energy storage systems due to their high energy density and long cycle life.[1] Lithium manganese oxide ($LiMn_2O_4$) with a spinel structure has been considered one of the promising cathode materials for rechargeable lithium batteries, owing to its low cost, environmental friendliness, high voltage operation and high safety. However, stoichiometric $LiMn_2O_4$ materials exhibit large capacity fade on cycling because of the Jahn-Tell distortion of trivalent Mn ions and the dissolution of Mn into the liquid electrolyte, especially at elevated temperature.[2-6] In order to overcome these problems, several cationic substitutions to produce $LiMn_{2-y}M_yO_4$ (M =Cr, Fe, Co, Ni, and Cu) have been studied in the literature.[7-13] Among these materials, $LiMn_{1.5}Ni_{0.5}O_4$ is of great interest as a cathode material for 5 V lithium-ion cells because of its high specific capacity and its dominant plateau at around 4.7 V, which arise from the presence of a Ni^{2+}/Ni^{4+} redox pair.[14-17] Various synthetic methods such as sol-gel, molten salt, co-precipitation and composition emulsion drying have been applied to the preparation of cathode active materials for lithium-ion batteries. The co-precipitation method is known as a simple way to prepare fine, highly pure and homogeneous powders of single or multi-component oxide materials.[18-20]

In this study, we synthesize spinel $LiMn_{1.5}Ni_{0.5}O_4$ cathode powders using the co-precipitation method at different calcination condition in order to achieve the best electrochemical properties. We investigate the effect of the calcination temperature on the morphologies, crystalline structure and electrochemical properties of spinel $LiMn_{1.5}Ni_{0.5}O_4$ cathode powders.

Experimental

$LiMn_{1.5}Ni_{0.5}O_4$ cathode powders were synthesized by co-precipitation using oxalic acid. A stoichiometric amount of lithium acetate dihydrate [$Li(CH_3COO)\cdot 2H_2O$, Aldrich], manganese(II) acetate tetrahydrate [$Mn(CH_3COO)_2\cdot 4H_2O$, Aldrich] and nickel(II) acetate tetrahydrate [$Ni(CH_3COO)_2\cdot 4H_2O$, Aldrich] were dissolved in de-ionized water. The solution was stirred continuously under heating at 60 °C. The oxalic acid solution was added to the homogeneous solution drop by drop. The mole ratio of oxalic acid to metal was 5.0. The solution was stirred at 90 °C for 2 h and further dried overnight at 110 °C. The dried precipitate was preheated at 450 °C for 3 h to decompose the organic components. The precursor powders were calcined at different temperatures (700, 800, 850, 900, 950, 1000 °C) for 15 h in air atmosphere. The morphological characteristics of the $LiMn_{1.5}Ni_{0.5}O_4$ powders were investigated using scanning electron microscopy (SEM, JEOL JSM 6701). Energy dispersive spectroscopy (EDS) and elemental mapping were performed using the same instrument. Powder X-ray diffraction (XRD, Philips X'PERT MPD) using Cu Kα radiation was used to identify the crystalline phase of the $LiMn_{1.5}Ni_{0.5}O_4$ powders. The cathode was prepared by coating an N-methyl pyrrolidone (NMP)-based slurry containing $LiMn_{1.5}Ni_{0.5}O_4$ powder, poly(vinylidene fluoride) (PVdF) and super-P carbon (85:7.5:7.5 by weight) on an aluminum foil. The thicknesses of the electrodes ranged from 50 to 55 μm after roll pressing, and their active mass loading corresponded to a capacity of about 1.2 mAh cm^{-2}. The lithium electrode consisted of a 150 μm-thick lithium foil that was pressed onto a copper current collector. A CR2032-type coin cell composed of lithium anode, a polypropylene separator (Celgard 2400) and $LiMn_{1.5}Ni_{0.5}O_4$ cathode was assembled with an electrolyte solution. The liquid electrolyte used in this study was 1 M $LiPF_6$ in ethylene carbonate (EC)/dimethyl carbonate (DMC) (1:1 by volume, battery grade, Soulbrain Co. Ltd.). All cells were assembled in a dry box filled with argon gas. Charge and discharge cycling tests of the Li/$LiMn_{1.5}Ni_{0.5}O_4$ cells were conducted at different current density over a voltage range of 3.0-4.9 V with battery testing equipment at room temperature.

Results and Discussion

The $LiMn_{1.5}Ni_{0.5}O_4$ powders with different morphologies were prepared by co-precipitation method with oxalic acid at different calcination temperatures. The effect of the calcination temperature on the morphologies of the $LiMn_{1.5}Ni_{0.5}O_4$ powders is shown in Figure 1. The $LiMn_{1.5}Ni_{0.5}O_4$ powders calcined at 700 °C exhibited nano-rod morphologies and aggregation of the powders, whereas powders calcined at 800 °C exhibited a well-faced crystallized spinel phase instead of a rod shape. As the calcination temperature increased, the particle size increased and the particle shape and distribution became more uniform. However, the particles calcined at 1000 °C had a larger size of several microns with aggregated morphologies between the particles. As a result, the $LiMn_{1.5}Ni_{0.5}O_4$ powders calcined at temperature ranges of 800 to 900 °C are well-distributed crystalloids with little agglomeration.

Figure 2 shows the XRD patterns of the $LiMn_{1.5}Ni_{0.5}O_4$ cathode powders calcined at different temperatures. The crystalline phase of all the powders can be identified to be a spinel structure indexed by cubic *Fd3m* in which lithium ions occupy the tetragonal (8a) sites, transition metals (Mn and Ni) are located at the octahedral (16d) sites, and oxygen atoms reside in 32e sites.[21] This indicates that the Mn site in the $LiMn_2O_4$ is partially substituted by Ni. Scherrer's formula given in Eq. (1) was used to determine the mean crystallite size (t) of the powder:

$$t = (0.94\,\lambda)/(B\cos\theta_B) \quad (1)$$

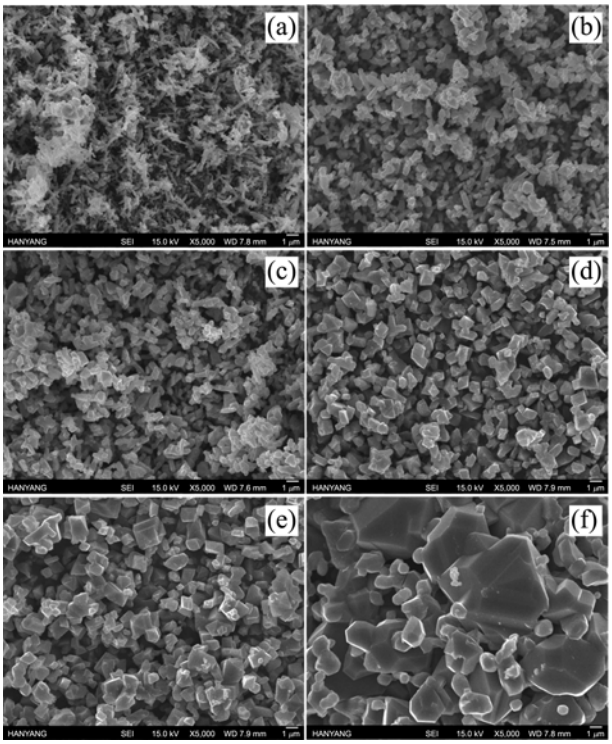

Figure 1. SEM images of $LiMn_{1.5}Ni_{0.5}O_4$ powders obtained at different calcination temperatures. (a) 700, (b) 800, (c) 850, (d) 900, (e) 950 and (f) 1000 °C.

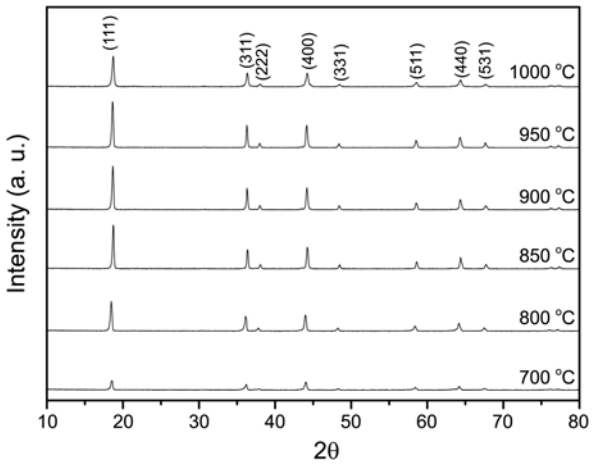

Figure 2. XRD patterns of $LiMn_{1.5}Ni_{0.5}O_4$ powders prepared at different calcination temperatures.

where λ is the wavelength of the X-ray used, θ_B is the Bragg angle of the diffraction peak considered, and B is the width at an intensity equal to half of the maximum intensity.[22] When the calcination temperature was increased from 700 to 1000 °C , the mean crystallite size of the cathode powders increased from 28 to 35 nm. By increasing the calcination temperature, the peak widths of the $LiMn_{1.5}Ni_{0.5}O_4$ powders become narrower and the relative intensities of the characteristic peaks gradually increase, indicating that a better crystalline structure of $LiMn_{1.5}Ni_{0.5}O_4$ was obtained. However, some very tiny peaks are observed around 37.5, 43.7 and 63.6°, which correspond to the weak impurity phases of $Li_xNi_{1-x}O$.[23,24] According to the previous reports,[25] $LiMn_{1.5}Ni_{0.5}O_4$ can loss oxygen and disproportionate to a mixture of a spinel phase and a secondary phase $Li_xNi_{1-x}O$ because of partial reduction of Mn^{4+} to Mn^{3+} at elevated temperature. Thus, the formation of the $Li_xNi_{1-x}O$ phase may result in a decrease of the Ni content and the Mn valence in the spinel phase. This result indicates that heat treatment at higher temperature results in more oxygen deficiency,

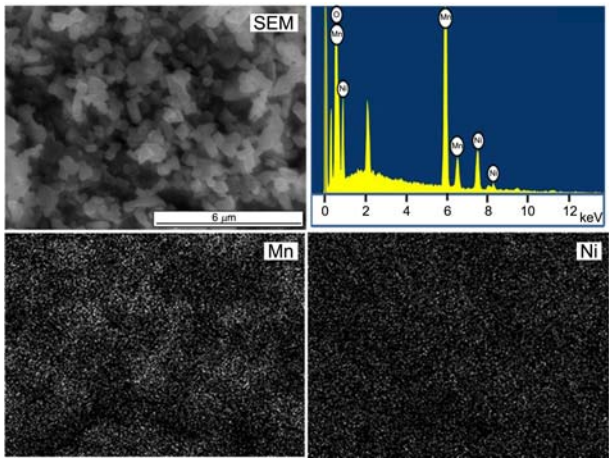

Figure 3. EDS spectrum of $LiMn_{1.5}Ni_{0.5}O_4$ powders calcined at 850 °C, and dot mappings for the Mn and Ni atoms in the corresponding $LiMn_{1.5}Ni_{0.5}O_4$ powders.

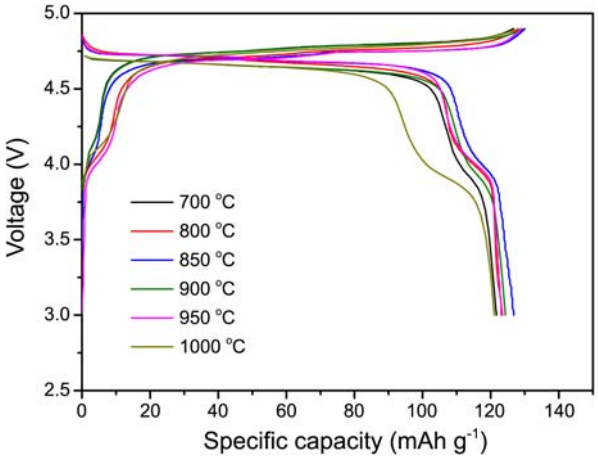

Figure 4. Initial charge and discharge curves of $LiMn_{1.5}Ni_{0.5}O_4$ cathode materials obtained at different calcination temperatures (0.5C rate, cut-off voltage: 3.0-4.9 V).

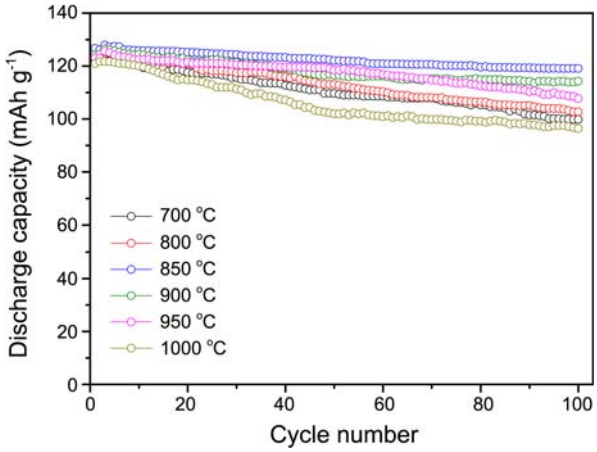

Figure 5. Discharge capacities of $LiMn_{1.5}Ni_{0.5}O_4$ cathode materials as a function of cycle number (0.5C rate, cut-off voltage: 3.0-4.9 V).

formation of Mn^{3+} and the occurrence of a secondary phase.

Figure 3 shows the EDS spectrum and dot mapping images of the $LiMn_{1.5}Ni_{0.5}O_4$ cathode powders calcined at 850 °C. In the dot mapping, the Mn and Ni components were observed to be well-dispersed inside the submicron-sized $LiMn_{1.5}Ni_{0.5}O_4$ powders. From the EDS spectrum shown in figure, the atomic ratio of manganese and nickel was calculated to be about 3.01:1, which is consistent with the chemical composition of the $LiMn_{1.5}Ni_{0.5}O_4$ powders.

Figure 4 shows the initial charge and discharge curves of $LiMn_{1.5}Ni_{0.5}O_4$ cathode materials calcined at different temperatures. The Li/$LiMn_{1.5}Ni_{0.5}O_4$ cells were subjected to charge and discharge cycling in the voltage range of 3.0-4.9 V at a constant current rate of 0.5C. The initial discharge capacities of $LiMn_{1.5}Ni_{0.5}O_4$ active materials ranged from 122 to 126 mAh g^{-1}, depending on the calcination temperature. The highest discharge capacity (126 mAh g^{-1}) was delivered by $LiMn_{1.5}Ni_{0.5}O_4$ powders calcined at 850 °C. Discharge capacities *vs* cycle number of the $LiMn_{1.5}Ni_{0.5}O_4$ cathode materials between 3.0 and 4.9 V are shown in Figure 5. $LiMn_{1.5}Ni_{0.5}O_4$ cathode material obtained at 850 °C exhibited high discharge capacity and good capacity retention (93% of initial discharge capacity after 100 cycles). As explained earlier, high calcination temperature may result in oxygen loss, Ni deficiency of $LiMn_{1.5}Ni_{0.5}O_4$ and formation of $Li_xNi_{1-x}O$ impurities,[24] which decrease the discharge capacity and deteriorate the cycling stability of the spinel $LiMn_{1.5}Ni_{0.5}O_4$ materials calcined at temperature higher than 850 °C. On the other hand, the integrated crystalline phase for structural stability is not well formed when the calcination temperature is below 850 °C. As a result, the discharge capacities are low in the $LiMn_{1.5}Ni_{0.5}O_4$ materials calcined at temperature lower than 850 °C. It is well known that the dissolution of transition metals suffering from unavoidable HF in electrolyte and the formation of LiF on the surface of cathode materials due to the electrolyte decomposition are mainly responsible for the capacity loss of electrode materials during cycling.[25-28] When the calcination temperature is

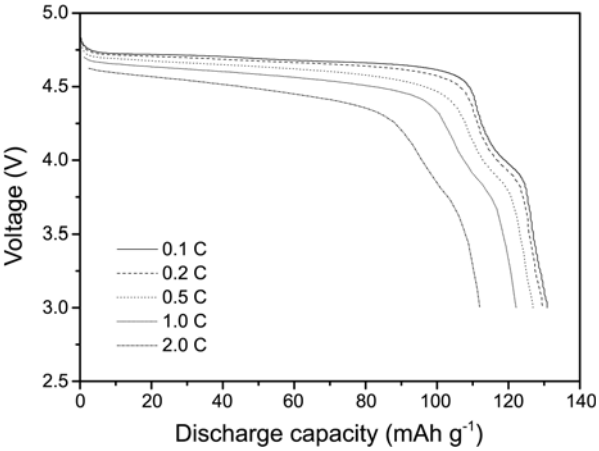

Figure 6. Discharge curves of the $LiMn_{1.5}Ni_{0.5}O_4$ cathode materials prepared at 850 °C, as a function of the C rate. The charging current rate was 0.1C with a 4.9 V cut-off.

below 850 °C, the $LiMn_{1.5}Ni_{0.5}O_4$ cathode materials have smaller particle size and larger specific surface area, thus higher dissolution of transition metals and electrolyte oxidation rate on its surface can be expected during cycling. Accordingly, the capacity retention behaviors of $LiMn_{1.5}Ni_{0.5}O_4$ cathode materials obtained at 700 and 800 °C are not as good as that of $LiMn_{1.5}Ni_{0.5}O_4$ obtained at 850 °C. As a result, the $LiMn_{1.5}Ni_{0.5}O_4$ cathode materials calcined at 850 °C exhibited the best electrochemical performance in consideration of discharge capacity and capacity retention.

We evaluated the rate capability of the $LiMn_{1.5}Ni_{0.5}O_4$ cathode materials obtained at different temperatures. The Li/$LiMn_{1.5}Ni_{0.5}O_4$ cells were charged to 4.9 V at a constant current rate of 0.1C and discharged at different current rates ranging from 0.1 to 2.0C. The discharge curves of the $LiMn_{1.5}Ni_{0.5}O_4$ cathode materials obtained at 850 °C are shown in Figure 6. Both voltage and discharge capacity decreased gradually as current rate increased. At 2.0C rate, the cell delivered a relatively high discharge capacity of 112 mAh g^{-1}. Figure 7 compares the relative discharge capacities of $LiMn_{1.5}Ni_{0.5}O_4$ cathode materials obtained at different

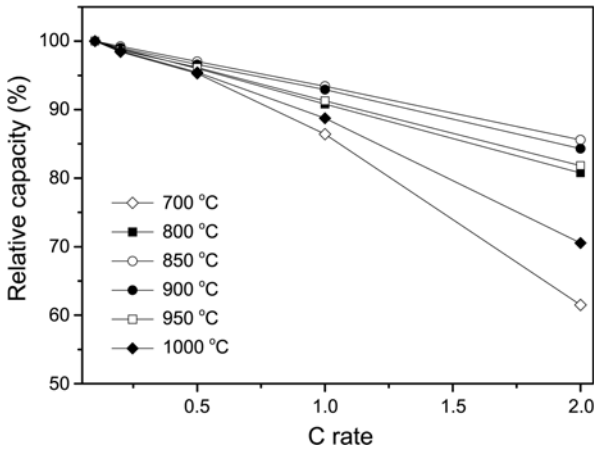

Figure 7. Relative capacities of $LiMn_{1.5}Ni_{0.5}O_4$ cathode materials prepared at different calcination temperatures, as a function of the C rate.

calcination temperatures, as a function of the C rate. The relative capacity is defined as the ratio of the discharge capacity at a specific C rate to the discharge capacity delivered at 0.1C rate. This result shows that the calcination temperature also affects the high rate performance. At a discharge rate of 2C, the $LiMn_{1.5}Ni_{0.5}O_4$ cathode materials obtained from 700, 800, 850, 900, 950 and 1000 °C delivered relative capacities of 61, 81, 86, 84, 82 and 71%, respectively. As for $LiMn_{1.5}Ni_{0.5}O_4$ cathode materials obtained below 850 °C, their lower crystallinity may be detrimental to their high rate performance. Moreover, smaller particle size with large specific surface area may give more chances to side reactions such as Mn^{3+} dissolution in the electrolyte. On the other hand, the $LiMn_{1.5}Ni_{0.5}O_4$ cathode materials calcined at high temperature have longer diffusion path for the intercalation and deintercalation of lithium ions, which deteriorate their cycling performance at high current rates. Hence, the $LiMn_{1.5}Ni_{0.5}O_4$ cathode materials calcined at 850 °C exhibited the best high rate performance, which can be ascribed to their fine size and well-defined crystalline structure.

Conclusion

$LiMn_{1.5}Ni_{0.5}O_4$ cathode powders were prepared at different calcination temperatures using the co-precipitation method. We investigated the effect of the calcination temperature on the morphologies, crystalline structure and electrochemical properties of the $LiMn_{1.5}Ni_{0.5}O_4$ powders. The $LiMn_{1.5}Ni_{0.5}O_4$ powders obtained from 800 to 900 °C showed a well-crystallized spinel phase and uniform shape with fine size. The $LiMn_{1.5}Ni_{0.5}O_4$ cathode materials calcined at 850 °C delivered the highest discharge capacities and exhibited good cycling characteristics in terms of the capacity retention and rate capability.

Acknowledgments. This work was supported by the National Research Foundation of Korea Grant funded by the Korean government (MEST) (NRF-2009-0092780 and NRF-2009-C1AAA001-0093307) and the Human Resources Development of KETEP Grant funded by the Korea government Ministry of Knowledge Economy (No. 20104010100560).

References

1. Tarascon, J.-M.; Armand, M. *Nature* **2001**, *414*, 359.
2. Thackeray, M. M.; Shao-Horn, Y.; Kahaian, A. J.; Kepler, K. D.; Skinner, E.; Vaughey, J. T.; Hackney, S. A. *Electrochem. Solid-State Lett.* **1987**, *1*, 7.
3. Inoue, T.; Sano, M. *J. Electrochem. Soc.* **1983**, *145*, 3704.
4. Amatucci, G. G.; Pereira, N.; Zheng, T.; Tarascon, J.-M. *J. Electrochem. Soc.* **2001**, *148*, A171.
5. Yamane, H.; Inoue, T.; Fujita, M.; Sano, M. *J. Power Sources* **2001**, *99*, 60.
6. Wu, H. M.; Tu, J. P.; Yuan, Y. F.; Li, Y.; Zhao, X. B.; Cao, G. S. *Mater. Chem. Phys.* **2005**, *93*, 461.
7. Amine, K.; Tukamoto, H.; Yasuda, H.; Fujita, Y. *J. Electrochem. Soc.* **1996**, *143*, 1607.
8. Ohzuku, T.; Takeda, S.; Iwanaga, M. *J. Power Sources* **1999**, *81*, 90.
9. Park, Y. J.; Lee, J. W.; Lee, Y. G.; Kim, K. M.; Kang, M. G.; Lee, Y. *Bull. Korean Chem. Soc.* **2007**, *28*, 2226.
10. Park, S. H.; Kang, S. H.; Johnson, C. S.; Amine, K.; Thackeray, M. M. *Electrochem. Commun.* **2007**, *9*, 262.
11. Kunduraci, M.; Amatucci, G. G. *Electrochim. Acta* **2008**, *55*, 4193.
12. Liu, D.; Han, J.; Goodenough, J. B. *J. Power Sources* **2010**, *195*, 2918.
13. Jin, Y.-C.; Lin, C.-Y.; Duh, J.-G. *Electrochim. Acta* **2012**, *69*, 45.
14. Idemoto, Y.; Sekine, H.; Ui, K.; Koura, N. *Solid State Ionics* **2005**, *176*, 299.
15. Kunduraci, M.; Al-Sharab, J. F.; Amatucci, G. G. *Chem. Mater.* **2006**, *18*, 3585.
16. Patoux, S.; Sannier, L.; Lignier, H.; Reynier, Y.; Bourbon, C.; Jouanneau, S.; Cras, F. L.; Martinet, S. *Electrochim. Acta* **2008**, *53*, 4137.
17. Sun, Y.; Yang, Y.; Zhan, H.; Shao, H.; Zhou, Y. *J. Power Sources* **2010**, *195*, 4322.
18. Kim, J. H.; Myung, S. T.; Sun, Y. K. *Electrochim. Acta* **2004**, *49*, 219.
19. Yi, T.-F.; Shu, J.; Zhu, Y.-R.; Zhou, A.-N.; Zhu, R.-S. *Electrochem. Commun.* **2009**, *1*, 91.
20. Liu, G. Q.; Wen, L.; Liu, G. Y.; Tian, Y. W. *J. Alloy Compd.* **2010**, *501*, 233.
21. Thackeray, M. M.; David, W. I. F.; Bruce, P. G.; Goodenough, J. B. *Mater. Res. Bull.* **1983**, *18*, 461.
22. Cullity, B. D. *Elements of X-ray Diffraction*, 2nd ed.; Addison-Wesley: Reading, MA, 1978; p 102.
23. Zhong, Q.; Bonakdarpour, A.; Zhang, M.; Gao, Y.; Dahn, J. R. *J. Electrochem. Soc.* **1997**, *144*, 205.
24. Fang, H.; Wang, Z.; Zhang, B.; Li, X.; Li, G. *Electrochem. Commun.* **2007**, *9*, 1077.
25. Ooms, F. G. B.; Kelder, E. M.; Schoonman, J.; Wagemaker, M.; Mulder, F. M. *Solid State Ionics* **2002**, *152-153*, 143.
26. Sun, Y. K.; Hong, K. J.; Prakash, J.; Amine, K. *Electrochem. Commun.* **2002**, *4*, 344.
27. Sun, Y. K.; Yoon, C. S.; Oh, I. H. *Electrochem. Acta* **2003**, *48*, 503.
28. Choi, N. S.; Yeon, J. T.; Lee, Y. W.; Han, J. G.; Lee, K. T.; Kim, S. S. *Solid State Ionics* **2012**, *219*, 41.